Electronic Supplementary Information

Green synthesis of poly ε-caprolactone using a metal-free catalyst via non-covalent interaction

Shweta Sagar, Priyanku Nath, Shiva Lall Sunar, Aranya Ray, Mridula, Alok Sarkar,* Saurabh K. Singh* and Tarun K. Panda*

Table of Contents

1. **Figure FS1- FS2.** ^{1}H, ^{13}C, NMR of N^1, N^2-dibutyl-N^1, N^1, N^2, N^2-tetramethylethane-1,2-diaminium bromide (**1**)
2. **Figure FS3.** First-order kinetics plots for CL polymerizations with time in $CDCl_3$ (1 mL) with different concentration of salt **1** at 60 ^{0}C
3. **Figure FS4.** Kinetics plots of ln [**1**] versus ln k_{obs} for the polymerization of CL in $CDCl_3$ (1 mL) at 60 ^{o}C
4. **Figure FS5.** Kinetics plots of [**1**] versus k_{obs} for the polymerization of CL in $CDCl_3$ (1 mL) at 60 ^{o}C
5. **Figure FS6.** First-order kinetics plots for CL polymerizations with time in $CDCl_3$ (1 mL) with different temperatures catalysed by salt **1**
6. **Figure FS7.** Eyring plot of ln(k_{obs} /T) ($Mm^{-1}K^{-1}$) vs (1/T) (K^{-1}) for (**1**) for the polymerization of CL with [CL]:[**1**] (100:1)
7. **Figure FS8.** Arrhenius plots of ln(k_{obs}) (Mm^{-1}) vs (1/T) (K^{-1}) for (**1**) for the polymerization of CL with [CL]:[**1**] (100:1)
8. **Table TS1.** ROP of ε-caprolactone by salt **1**
9. **Figure FS9.** Plot of theoretical, experimental M_n and molecular weight distribution of PLA as functions of molar equivalent of CL with respect to salt **1** (M_n = number average molecular weight, PDI = polydispersity index)
10. **Figure FS10.** ^{1}H NMR spectrum (400 MHz, 25°C, $CDCl_3$) of PCL (Entry 4, Table TS1)
11. **Figure FS11.** ^{13}C NMR spectrum (100 MHz, 25°C, $CDCl_3$) of PCL (Entry 4, Table TS1)
12. **Figure FS12.** GPC profile of PCL sample (Entry 4, Table TS1)
13. **Table TS2.** Recovery of solvent during the ROP of ε-CL
14. **Table TS3.** Recyclability of the catalyst up to six consecutive cycles.
15. **Table TS4.** Influence of the solvent on the ROP of ε-CL initiated by salt 1
16. **Figure FS13.** Energy-dispersive X-ray spectroscopy (EDAX) analysis for the PCL sample
17. **Table TS5.** Calculation of green metric parameters of our work
18. **Table TS6.** Calculation of green metric parameters of previous work
19. **Figure FS14.** Plots of electron deformation densities (EDD) corresponding to the highest interaction $\Delta E_{\mathbf{orb}}$ for complexes A and B
20. **Table TS7**. EDA-NOCV energies computed at B3LYP-D3BJ/TZP level of the theory for complexes **A** and **B**. All the values are in kcal/mol.
21. **Table TS8.** DFT optimized coordinates and the thermodynamic parameters.

General

Polymerization reactions were carried out in a dried Schlenk tube with a magnetic stirrer. In a typical procedure, first, the monomer (ε-caprolactone) (292 mg, 2.56 mmol) was added to the solution of **1** (10 mg, 0.026 mmol) in toluene (1 mL). Then, the solution was stirred at the required temperature for a desired reaction time, after which the solution was quenched by benzyl alcohol. The solution was concentrated in a vacuum, and the polymer was recrystallized from hexane, followed by methanol precipitation. The final polymer obtained was dried under vacuum to constant weight.

Synthesis of N, N'-dibutyl- N, N, N', N'-tetramethylethane-1, 2-diaminium bromide (DBTMEDA)Br_2 (1)

N^1, N^2-dibutyl-N^1, N^1, N^2, N^2-tetramethylethane-1,2-diaminium bromide (**1**) salt was synthesized using a procedure reported in the literature.[1] Yield: 1.61 g, 96%. ^{1}H NMR (600 MHz, DMSO-d_6) δ_H 3.96 (s, 4H, *J*= 3.96 Hz), 3.41-3.38 (t, 4H, *J*= 3.40 Hz), 3.17 (s, 12H, *J*= 3.17 Hz), 1.75-1.69 (m, 4H, *J*= 1.72 Hz), 1.36-1.29 (m, 4H, *J*= 1.33 Hz), 0.97-0.95 (t, 6H, *J*= 0.96 Hz). ^{13}C NMR (151 MHz, DMSO-d_6) δ_C 64.5, 55.4, 50.9, 39.9, 24.2, 19.6, 14.0.

GPC Analysis

GPC studies were carried out on a Waters GPC K13515581A instrument, with a flow rate of 1 mL min^{-1} in THF as a solvent. Universal calibration was carried out using polystyrene standards, laser light scattering detector data, and a concentration detector.

DSC Analysis

DSC studies were conducted on a SDT Q200 DSC instrument, with a heating rate of 10 ˚C min^{-1} under N_2 flow (50 ml min^{-1}). DSC technical indicators are as follows: maximal sensitivity, 0.2 mw; calorimeter accu*rac*y, before 1%; calorimeter precision, before 1%; temperature accuracy, < 0.1 ˚C; temperature precision, < 0.01 ˚C. An unsealed Al pan with a 2.0 mg sample was used in the experiments. For ΔH measurements, the DSC system was calibrated with indium (m.p. 156.60 ˚C; ΔH_{fus} = 28.45 J g^{-1}).

TGA analysis

TGA analysis was carried out using a SDT Q600 TGA instrument. TGA technical indicators are as follows: balance sensitivity, 0.1 mg; balance accu*rac*y, prior to 0.1%; balance precision, prior to 0.02%; weighting precision, reach to 10 ppm; temperature precision, ±2 ˚C (measure sample). TGA experiment was carried out under N_2 dynamic atmospheres at a flow rate of 10 mL min^{-1}. 2 mg PCL/P C-a sample was heated from 40 to 500 ˚C at 10 ˚C min^{-1} in a nitrogen atmosphere (50 ml min^{-1}).

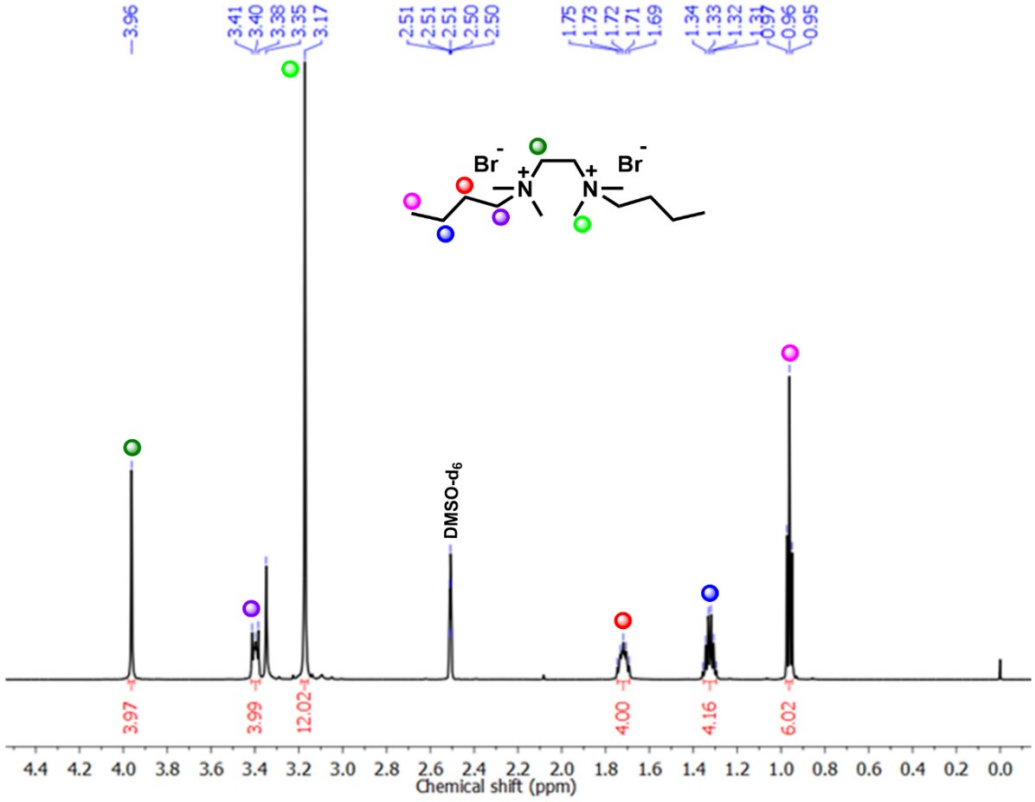

Figure FS1. ^{1}H-NMR (400 MHz, DMSO-d_6, 25 ˚C) of N^1, N^2-dibutyl-N^1, N^1, N^2, N^2-tetramethylethane-1,2-diaminium bromide (**1**).

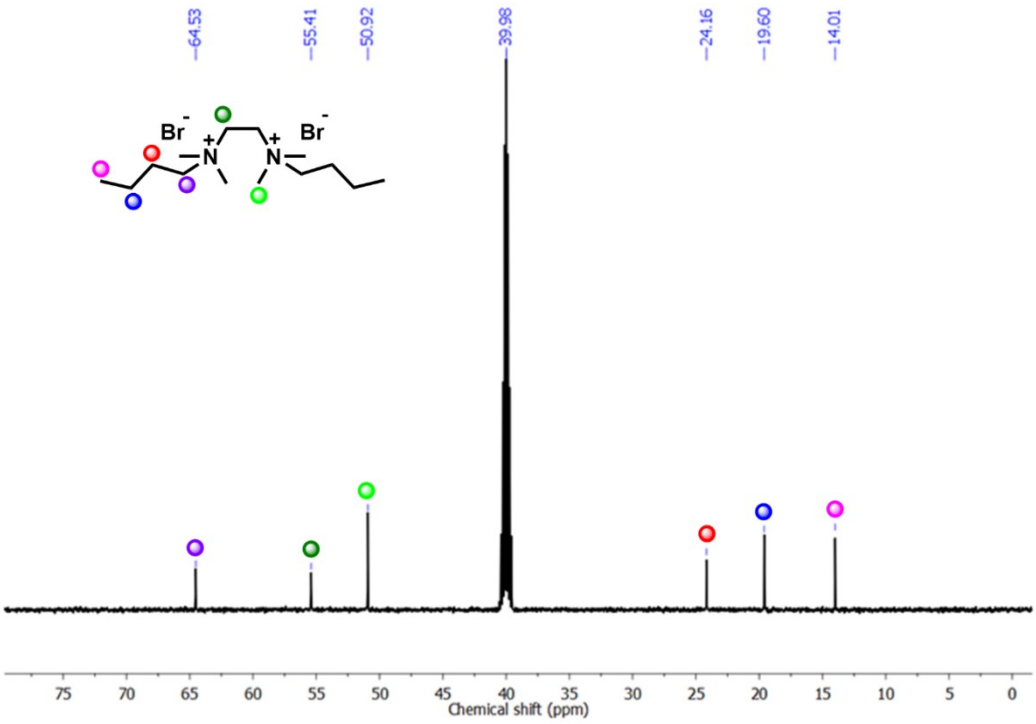

Figure FS2. ^{13}C-NMR (100 MHz, DMSO-d_6, 25 ˚C) of N^1, N^2-dibutyl-N^1, N^1, N^2, N^2-tetramethylethane-1,2-diaminium bromide (**1**).

Kinetics Study for ε-CL polymerization

We investigated the kinetics to understand the polymerization behavior. The kinetic plots of $[CL]_0/[CL]$ versus the catalyst (1) were found to be linear, indicating first-order dependence on ε- CL concentration (Figure FS3). The first-order dependence of the polymerization reactions substantiates the presence of only one initiator and, consequently, follows the second-order rate law, which can be expressed as rate = $-d[CL]/dt = k_p [cat]^1 [CL]^1$. The activation parameters for the ROP or ε-CL in $CDCl_3$ were found to be $\Delta H^{\ddagger}$= 10.8 kJmol^{-1}K^{-1} and $\Delta S^{\ddagger}$= -0.14 kJmol^{-1}K^{-1}, $\Delta Ea^{\ddagger}$ = 13.5 kJmol^{-1}. The $\Delta G^{\ddagger}$ value for the ring-opening polymerization of ε-CL catalyzed by **1** at 60°C was calculated to be 57.4 kJmol^{-1}. Therefore, the rate expression can be summarized as

$-d[CL]/dt = k_{app} [\mathbf{1}]^1 [CL]^1$ .....Equation 1

$-d[CL]/dt = k_{obs} [CL]^1$ .....Equation 2

where $k_{obs} = k_{app} [\mathbf{1}]^1$.

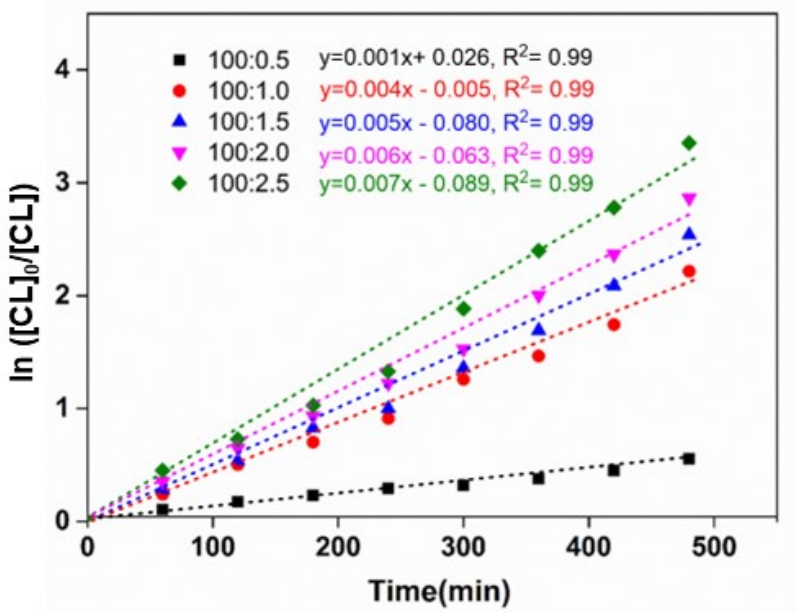

Figure FS3. First order kinetics plots for CL polymerizations with time in $CDCl_3$ (1 mL) with different concentration of salt **1** at 60 ^{0}C.

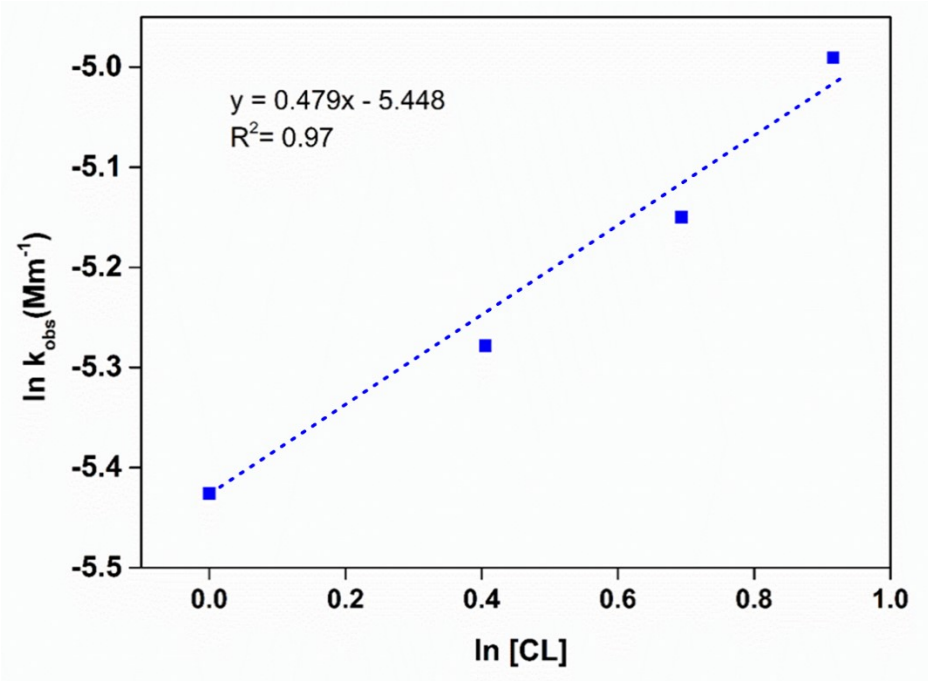

Figure FS4. Kinetics plots of ln [**1**] versus ln k_{obs} for the polymerization of CL in $CDCl_3$ (1 mL) at 60 ^{o}C.

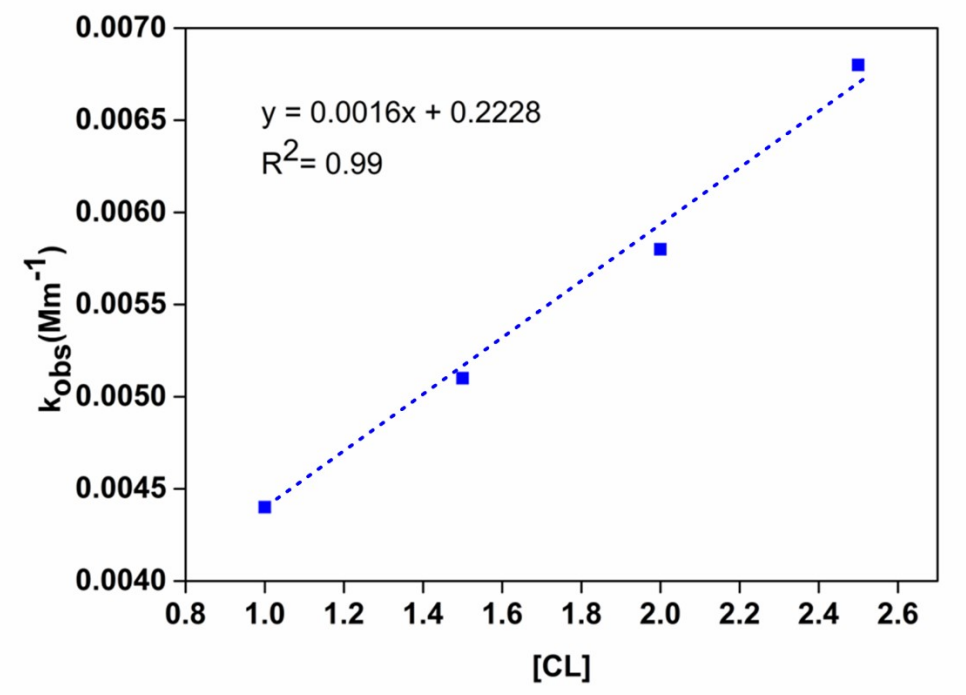

Figure FS5. Kinetics plots of [**1**] versus k_{obs} for the polymerization of CL in $CDCl_3$ (1 mL) at 60 °C.

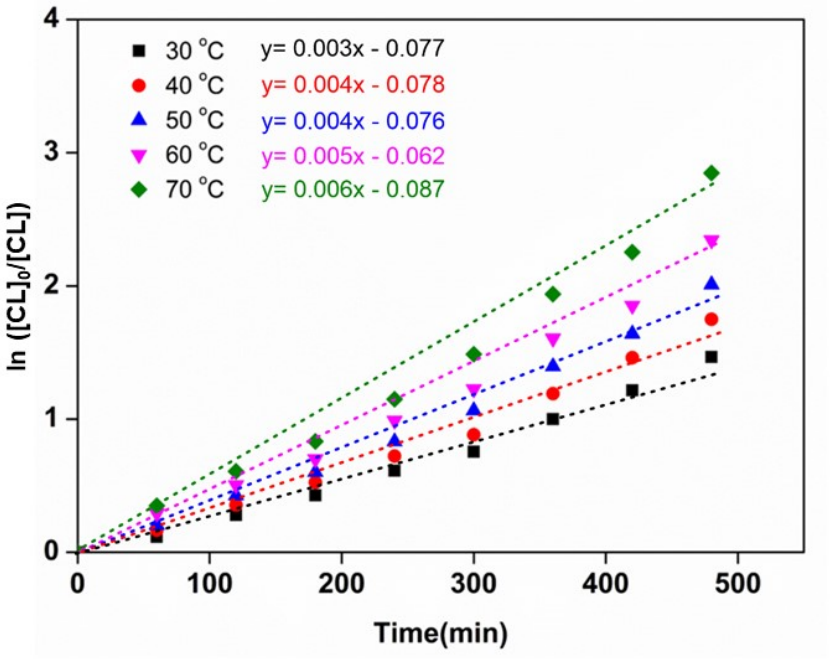

Figure FS6. First order kinetics plots for CL polymerizations with time in $CDCl_3$ (1 mL) with different temperatures catalysed by salt **1**.

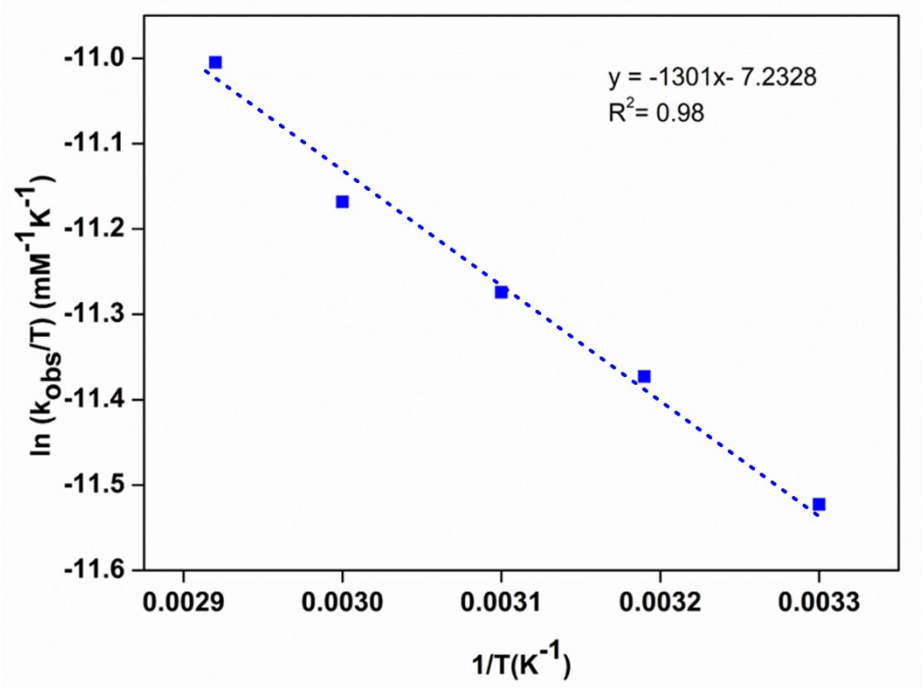

Figure FS7. Eyring plot of ln(k_{obs} /T) ($Mm^{-1}K^{-1}$) vs (1/T) (K^{-1}) for (**1**) for the polymerization of CL with [CL]:[**1**] (100:1).

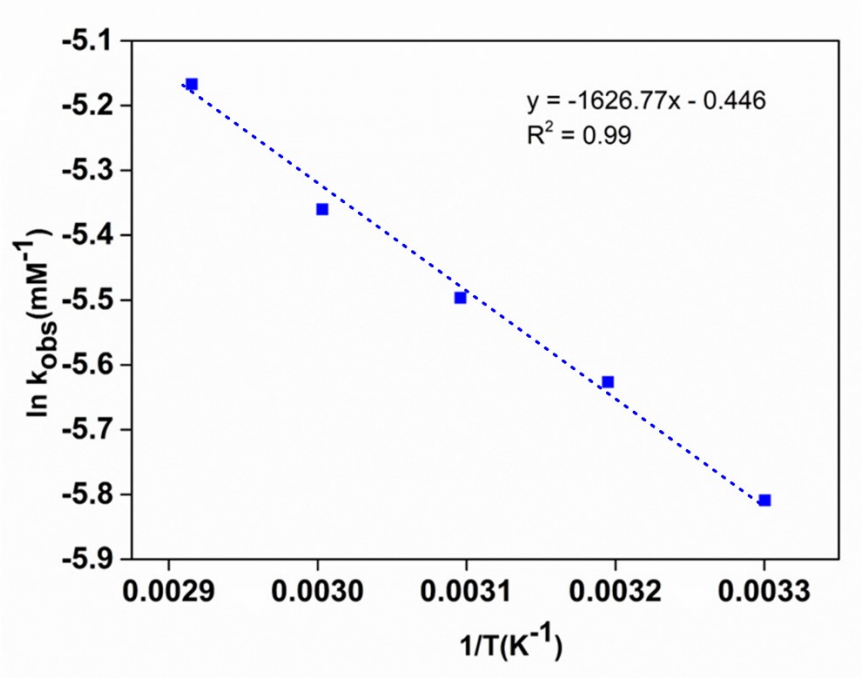

Figure FS8. Arrhenius plots of ln(k_{obs}) (Mm^{-1}) vs (1/T) (K^{-1}) for (**1**) for the polymerization of CL with [CL]:[**1**] (100:1).

Eyring Equation:

$$\ln \frac{k}{T} = \frac{-\Delta H^{\ddagger}}{R} \cdot \frac{1}{T} + \ln \frac{k_B}{h} + \frac{\Delta S^{\ddagger}}{R}$$

Arrhenius Equation:

$$\ln k = \frac{-E_a}{R}\left(\frac{1}{T}\right) + \ln A$$

Where,

- k_B is the Boltzmann's constant (1.381 x 10^{-23} J/K)
- T is the absolute temperature in Kelvin (K)
- h is Planck's constant (6.626 x 10^{-34} Js)
- $\Delta H^{\ddagger}$ is **enthalpy of activation** (J/(mol K)
- $\Delta S^{\ddagger}$ is **entropy of activation** (J/(mol K)
- $\Delta E_a^{\ddagger}$ is activation energy (J/(mol K)
- $\Delta G^{\ddagger}$ is Gibbs energy of activation (J/mol)
- R is Gas constant (8.314 J/K mol)

Table TS1. ROP of ε-caprolactone by salt **1**.[a]

Entry	Cat:M	Time (h)	Temp (˚C)	Conv[b]	Yield[c]	M_{ntheo}[d] (*k*Da)	M_{nexp}[e] (*k*Da)	PDI
1	1:100	2	60	37.6	21	4.4	3.1	1.6
2	1:100	4	60	58.8	48	6.8	5.9	1.4
3	1:100	6	60	79.9	81	9.2	8.8	1.3
4	1:100	8	60	98.3	99	11.3	11.0	1.1
5	1:200	8	60	98.1	99	22.5	21.9	1.1
6	1:300	8	60	97.8	98	33.6	33.1	1.2
7	1:400	8	60	96.7	97	44.3	43.5	1.2
8	1:500	8	60	95.5	96	54.6	51.6	1.4
9	0:100	8	60	0	0	-	-	-
10[f]	1:100	8	60	22.5	14	nd	nd	nd

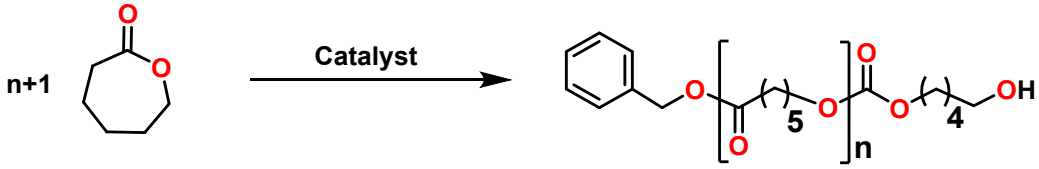

[a]In toluene, [Salt] = 0.026 mmol, 0.04 M, [b]Conversions were determined by crude mixture ^{1}H NMR spectroscopy. [C](weight of the polymer obtained/ weight of monomer used)*100. [d]$M_{n\ (theo)}$ = molecular weight of chain-end + 114 gmol^{-1} × (Salt: M) × conversion. [e]In THF (2 mg mL^{-1}) and molecular weights were determined by GPC-LLS (flow rate = 0.5 mL min^{-1}). Universal calibration was carried out with polystyrene standards, laser light scattering detector data, and concentration detector. Each experiment is duplicated to ensure precision. [f]Absence of salt.

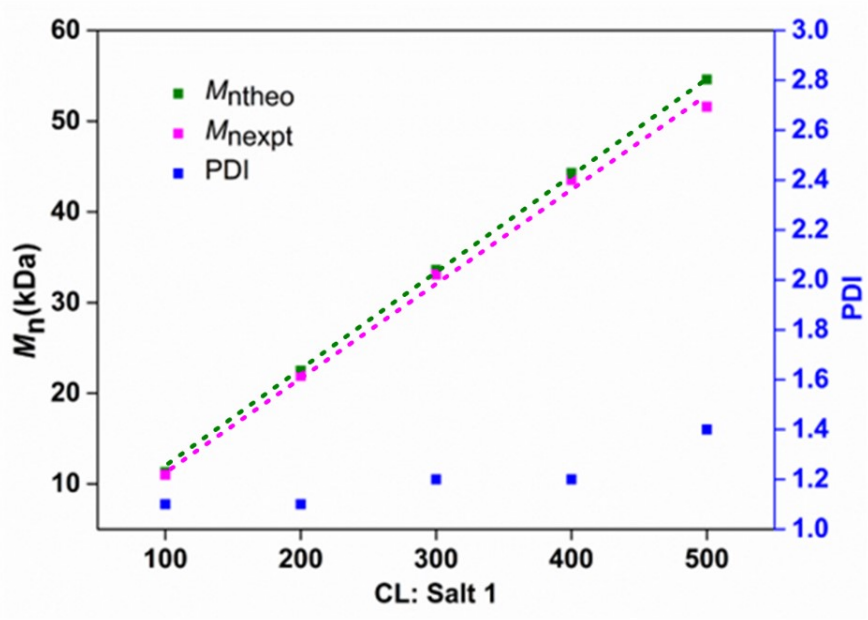

Figure FS9. Plot of theoretical, experimental M_n and molecular weight distribution of PLA as functions of molar equivalent of CL with respect to salt **1** (M_n = number average molecular weight, PDI = polydispersity index).

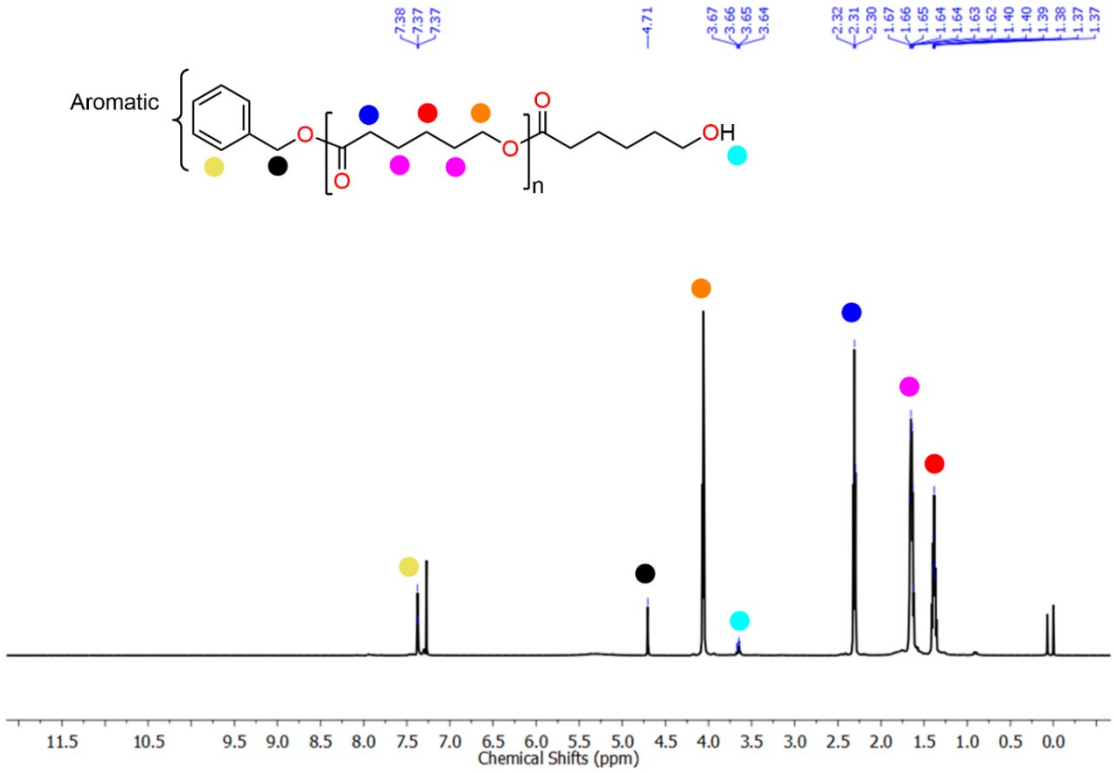

Figure FS10. ^{1}H NMR spectrum (400 MHz, 25°C, $CDCl_3$) of PCL (Entry 4, Table TS1).

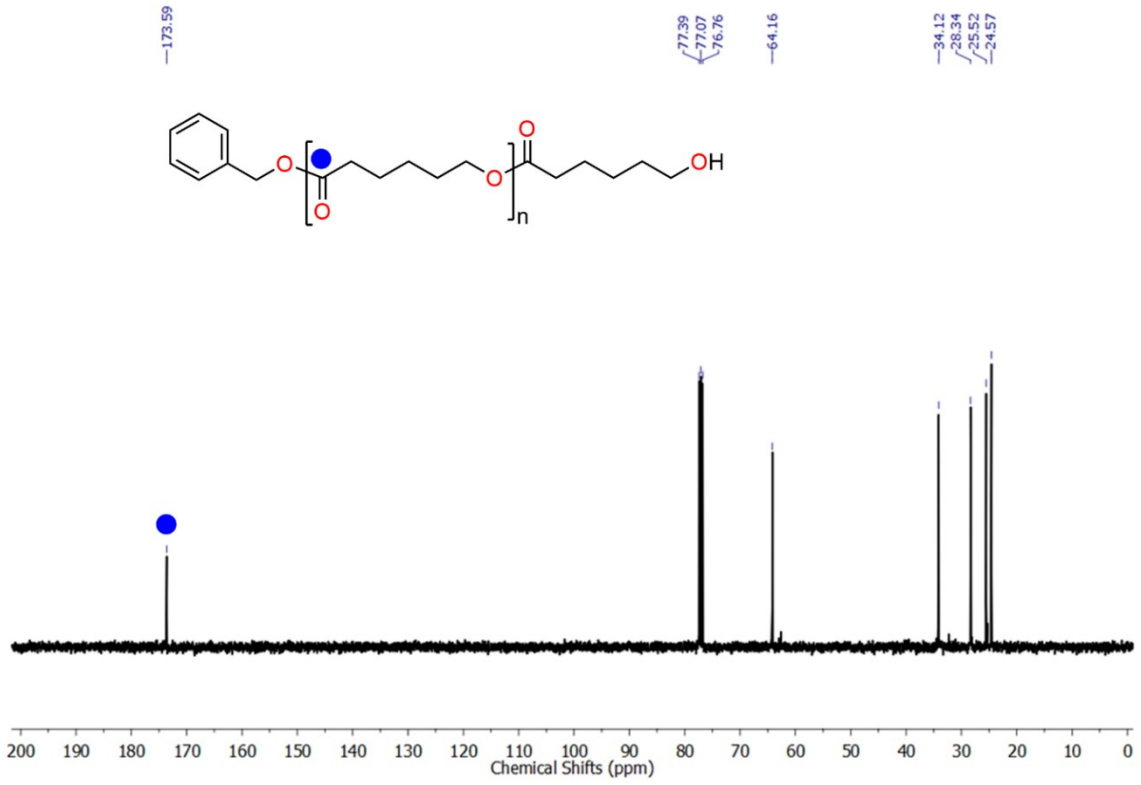

Figure FS11. ^{13}C NMR spectrum (100 MHz, 25°C, $CDCl_3$) of PCL (Entry 4, Table TS1).

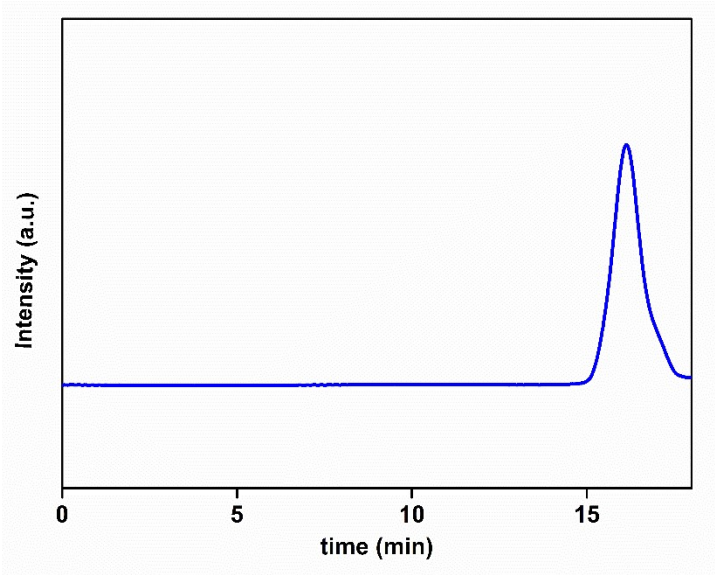

Figure FS12. GPC profile of PCL sample (Entry 4, Table TS1).

Solvent recovery experiment

The recovery of toluene used as a solvent was assessed in terms of its possible application in the industry. It was studied for the ROP of ε-CL (38.46 mmol) and catalyst (0.3846 mmol) under the standard reaction conditions. After the polymerization (8 h), the entire reaction mixture was added dropwise to the water, where the PCL was precipitated as a solid, and the catalyst was dissolved in water. We followed the standard workup procedure to separate toluene from water. We separated the toluene used for the reaction mixture by using a separating funnel. Initially, we added 10ml of toluene during the reaction and recovered around 9.5ml after workup for the first cycle.

Table TS2. Recovery of solvent during the ROP of ε-CL.

No of cycle	**Toluene added to the reaction**	**Toluene recovered after workup**	**Percentage of Toluene recovered**
1	10 ml	9.5 ml	95%

Recovery of the Catalyst:

Initially, we took 150 mg of catalyst. Catalyst recovery amount and yield obtained were as: Run 0 after 1st cycle (142 mg, 95%), Run 1 (133 mg, 94%), Run 2 (125 mg, 93%), Run 3 (115 mg, 92%), Run 4 (105 mg, 91%), Run 5 (85 mg, 80%).

Table TS3. Recyclability of the catalyst up to six consecutive cycles.

No of cycle	Amount of catalyst recovered (mg)	Percentage of catalyst recovered
1	142	95%
2	133	94%
3	125	93%
4	115	92%
5	105	91%
6	85	80%

Table TS4. Influence of the solvent on the ROP of ε-CL initiated by salt **1**[a].

Entry	Solvent	Conversion[b]	Yield[c]
1	Hexane	15	12
2	Ethanol	8	10
3	Acetonitrile	no conversion	-
4	Ethylacetate	no conversion	-

[a]Polymerization conditions: [Catalyst] = 0.026 mmol, desired solvent= 2 ml, [CL] = 2.56 mmol, [CL]: [**1**] = 100:1, 8 h, 60 ° C, [b]Conversions were determined by crude mixture ^{1}H NMR spectroscopy. [C](weight of the polymer obtained/ weight of monomer used)*100.

Element	Weight %	Atomic %	Net Int.	Error %	Kratio	Z	A	F
C K	78.72	93.75	3850.23	3.39	0.7153	0.7424	1.2239	1.0000
O K	5.73	5.12	184.65	10.69	0.0162	0.7113	0.3973	1.0000
AuL	15.55	1.13	57.02	11.21	0.0746	0.4647	1.0256	1.0073

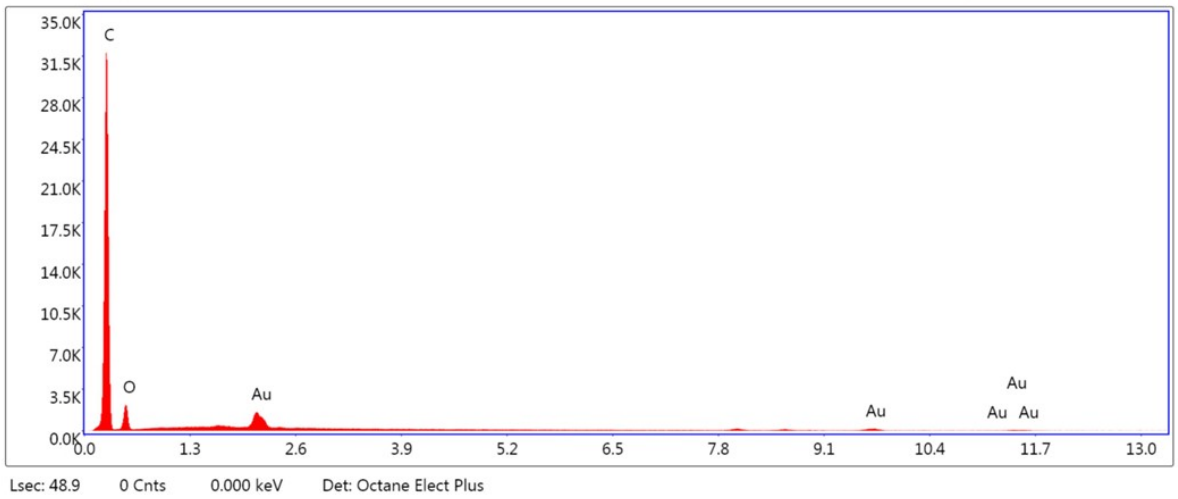

Figure FS13. Energy-dispersive X-ray spectroscopy (EDAX) analysis for the PCL sample (Entry 4, Table TS1).

Table TS5. Calculation of green metric parameters of our work

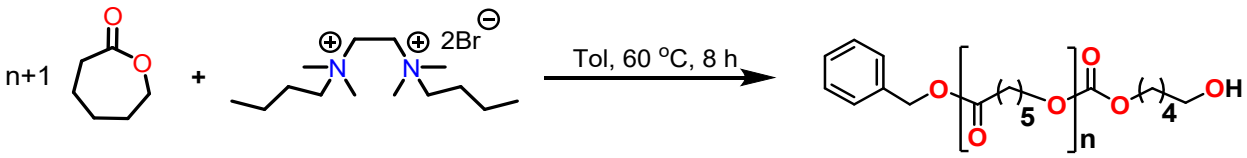

Entry	Description	Chemical formula	Molecular weight (g/mol)	No. of moles (mmol)	Amount (mg)
Reactant 1	ε-CL	$C_6H_{10}O_2$	114.14	2.56	292
Catalyst	Salt	$C_{14}H_{34}Br_2N_2$	390.25	0.026	10
Solvent	Toluene	C_7H_8	-	-	4.45
Product	PCL	-	11000	-	289

Yield of product: 99%

No. of repeating units, n = 96

Equivalent of monomer = 100

Equivalent of salt = 1

1. E-factor or environmental factor: It measures the mass of generated waste per unit mass of the product. The ideal value of the E - factor is zero.

E factor = Total mass of the waste /Mass of the product

Where the total mass of waste = total mass of raw materials – the total mass of product

E factor = {(114.14*2.56) – 289} / 289

= **0.01**

2. Atom economy (AE): It calculates how many atoms of the reactants are present in the final product. The ideal value of the AE factor is 100%.

Atom economy = {MW of product / Σ (MW of reactants)} × 100

= = {11000/ (114.14× 96)} × 100

= 100%

3. Atom efficiency = (% yield of product × % atom economy) / 100

= **99%**

4. Carbon efficiency = {No. of carbon atoms in the product / Σ (No of carbon atoms in reactants} × 100

= {(6 × 96) / (6 × 96)} × 100

= (576 / 576) × 100

= **100%**

5. Product mass intensity (PMI): PMI is defined as the total mass of the input materials (reactants), including solvent, in a chemical reaction divided by the mass of the product.

PMI = Σ (Mass of reactants including solvent) / Mass of the product

= 296.5 / 289

= **1.02**

Ideal value of **PMI = E factor + 1**

= 0.01 + 1 = **1.01**

6. Reaction mass efficiency (RME): RME is a mass-based metric which is defined as the mass of a product divided by the total mass of stoichiometric reactants. The value of RME varies from 0- 100%. It measures the percentage of the mass of reactants in the final product. The more RME values, the greener the reaction will be.

RME = {Mass of product/ Σ (mass of reactants)} × 100

= {289 / 292} × 100

= **98.9%**

Summarized green metric parameters

E-factor	0.01
AE	100%
Atom efficiency	99%
Carbon efficiency	100%
PMI	1.02
RME	98.9%

Table TS6. Calculation of green metric parameters from previous report

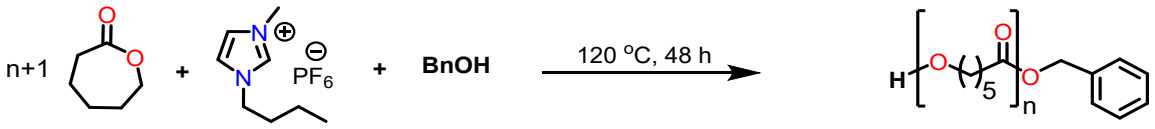

Entry	Description	Chemical formula	Molecular weight (g/mol)	No. of moles (mmol)	Amount (mg)
Reactant 1	ε-CL	$C_6H_{10}O_2$	114.14	100	11414
Catalyst	Ionic liquid	$C_8H_{15}F_6N_2F$	284.19	2	568.4
BnOH	Initiator	C_7H_8O	108.14	2	216.3
Product	PCL	-	7740	-	7740

Yield of product: 100%

No of repeating units, n = 68

Equivalent of monomer = 100

Equivalent of Ionic liquid = 1

Equivalent of BnOH = 1

1. E-factor or environmental factor: It measures the mass of generated waste per unit mass of the product. The ideal value of the E - factor is zero.

E factor = Total mass of the waste /Mass of the product

Where the total mass of waste = total mass of raw materials – the total mass of product

E factor = {(114.14*100) + (108.14*2) – 7740} / 7740

= **0.5**

2. Atom economy (AE): It calculates how many atoms of the reactants are present in the final product. The ideal value of the AE factor is 100%.

Atom economy = {MW of product / Σ (MW of reactants)} × 100

= {7740/ [(114.14× 68) +108.14]} × 100

= 98%

3. Atom efficiency = (% yield of product × % atom economy) / 100

= 98%

4. Carbon efficiency = {No. of carbon atoms in the product / Σ (No of carbon atoms in reactants} × 100

= {(6 × 68) + 7 / (6 × 68) + 7)} × 100

= **100 %**

5. Product mass intensity (PMI): PMI is defined as the total mass of the input materials (reactants), including solvent, in a chemical reaction divided by the mass of the product.

PMI = Σ (Mass of reactants) / Mass of the product

= (11630 / 7740)

= **1.5**

Ideal value of **PMI = E factor + 1**

= 0.5 + 1 = **1.5**

6. Reaction mass efficiency (RME): RME is a mass-based metric which is defined as the mass of a product divided by the total mass of stoichiometric reactants. The value of RME varies from 0- 100%. It measures the percentage of the mass of reactants in the final product. The more RME values, the greener the reaction will be.

RME = {Mass of product/ Σ (mass of reactants)} × 100

= {7740 / 11630} × 100

= **66%**

Summarized green metric parameters

E-factor	0.5
AE	98%
Atom efficiency	98%
Carbon efficiency	100%
PMI	1.5
RME	66%

Computational Details

Energy decomposition analysis (EDA) has been carried out using ADF 2021.106 code on complexes A and B to compute the interaction energy. The interaction energy is further decomposed into various contributions,

$$\Delta E_{int} = \Delta E_{elst} + \Delta E_{Pauli} + \Delta E_{orb} + \Delta E_{disp} \quad (1)$$

where the term ΔE_{elst} corresponds to the electrostatic interaction (attractive in nature), ΔEPauli refers to the Pauli repulsion energy, ΔE_{orb} orbital accounts for orbital interactions resulting from electron pair bonding, charge transfer, and polarization terms, and ΔE_{disp} represents the dispersion interaction terms. The computed total interaction energies (ΔE_{int}) are -38.3 and -31.1 kcal mol^{-1} for complex A and B, respectively. The computed intermolecular interactions are significantly large for structure A and as compared to structure B. EDA analysis reveals that both the electrostatic and Pauli interactions are significant contributors toward the total bonding energy, where the former is attractive in nature while the Pauli repulsion is repulsive in nature. In addition, we have also observed significant orbital contribution (ΔE_{orb}) to the total bonding energy, and the ΔE_{orb} values are -16.31 and -13.01 kcal/mol. For A and B, we noticed a marginal difference in the ΔE_{orb} values due to the difference in the interactions. Due to the strong interaction in A compared to B, the electrostatic and orbital interactions are larger, resulting in a relatively higher interaction energy for A (see Table S2). In complex B, the computed electrostatic contribution is nearly ~12 % smaller than what was observed for complex A. In addition, we have also noticed a decrease in the orbital contribution to the total interaction energy for B. In all the complexes, the dispersion interaction always stabilizes in nature and contributes around 14% of the total bonding energy in A and 10% of the total bonding energy in B.

The decomposed energy shows that the significant contribution emerges from electrostatic interactions, followed by Pauli (repulsive in nature) and orbital interactions. Due to hydrogen bonding interactions, we observed relatively higher electrostatic and orbital interaction energy in species **A** than in species **B.** The steric repulsion (Pauli) is relatively large in species **A**, due to the large number of protons close to the ε-CL. Moreover, the dispersion interactions are more robust in species A than in species B.

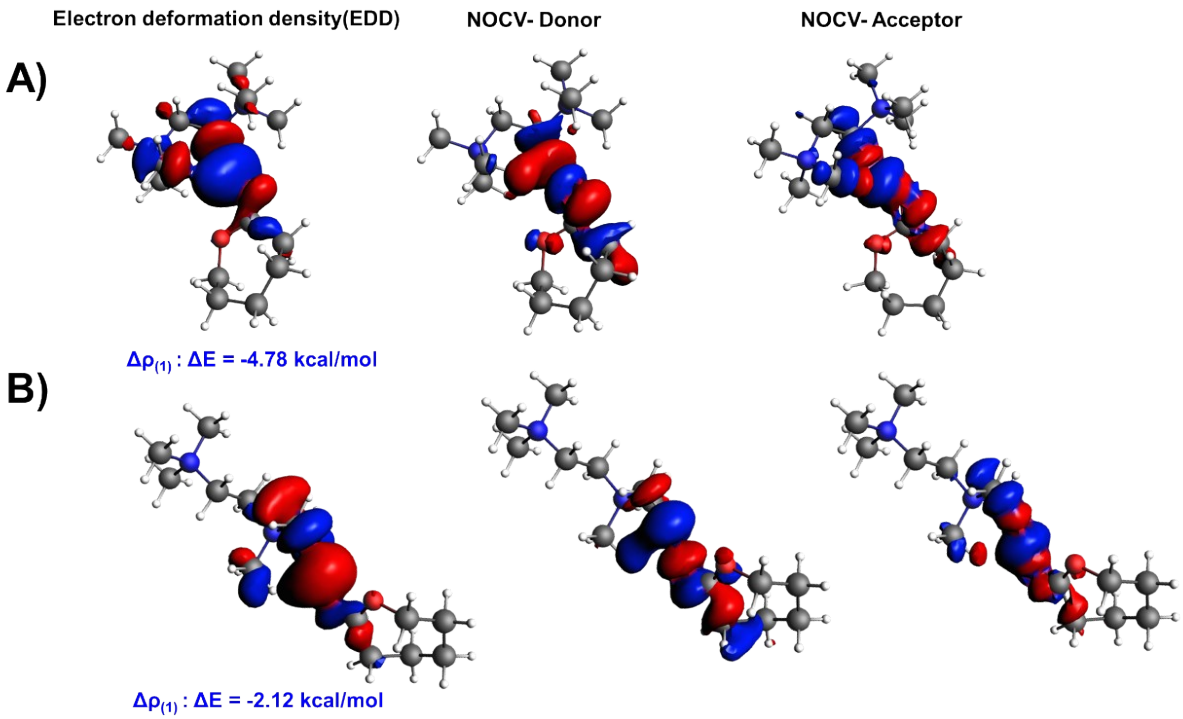

Figure FS14. Plots of electron deformation densities (EDD) corresponding to the highest interaction $\Delta E_{\mathbf{orb}}$ for complexes A and B.

Table TS7. EDA-NOCV energies computed at B3LYP-D3BJ/TZP level of the theory for complexes **A** and **B**. All the values are in kcal/mol.

Energy	**A**	**B**
ΔE_{int}	-38.32	-31.12
ΔE_{pauli}	19.38	16.63
ΔE_{disp}	-5.37	-3.27
$\Delta E_{elestat}$	-36.03	-31.47
ΔE_{orb}	-16.31	-13.01

Table TS8. DFT optimized coordinates and the thermodynamic parameters.

A

N	10.167966000000	-10.568660000000	-3.406612000000
N	10.167249000000	-13.272456000000	-6.075775000000
C	10.625247000000	-11.881989000000	-3.999469000000
H	11.641189000000	-12.042674000000	-3.621803000000
H	9.966103000000	-12.635542000000	-3.548724000000
C	10.610448000000	-11.934703000000	-5.524414000000
H	9.932203000000	-11.198266000000	-5.970196000000
H	11.608351000000	-11.749754000000	-5.938018000000
C	10.451218000000	-13.270644000000	-7.553047000000
H	11.530703000000	-13.212249000000	-7.711992000000
H	10.063547000000	-14.196337000000	-7.983389000000
H	9.952793000000	-12.413882000000	-8.013269000000
C	10.924206000000	-14.405958000000	-5.440477000000
H	10.579779000000	-14.549732000000	-4.412980000000
H	10.715431000000	-15.313702000000	-6.011237000000
H	11.994966000000	-14.188103000000	-5.480441000000
C	10.336028000000	-10.685029000000	-1.912368000000
H	11.392619000000	-10.845360000000	-1.685300000000
H	9.997076000000	-9.753780000000	-1.453554000000
H	9.729337000000	-11.525436000000	-1.565106000000
C	10.997377000000	-9.423084000000	-3.902163000000
H	12.050331000000	-9.627306000000	-3.690615000000
H	10.843858000000	-9.286667000000	-4.975130000000
H	10.687935000000	-8.514420000000	-3.380391000000
C	8.692445000000	-13.479657000000	-5.866355000000
H	8.150186000000	-12.698862000000	-6.406502000000
H	8.427306000000	-14.457963000000	-6.274428000000
H	8.464285000000	-13.459740000000	-4.795624000000
C	8.712198000000	-10.319083000000	-3.682227000000

H	8.550556000000	-10.184366000000	-4.753839000000
H	8.138788000000	-11.167201000000	-3.297699000000
H	8.420522000000	-9.400330000000	-3.168087000000
C	8.131502000000	-14.498919000000	-2.184877000000
C	7.281332000000	-14.764291000000	-0.982260000000
C	5.929773000000	-15.412871000000	-1.327771000000
C	6.007533000000	-16.912637000000	-1.568547000000
C	6.907710000000	-17.313821000000	-2.728604000000
C	8.353232000000	-16.898825000000	-2.573152000000
O	8.591111000000	-15.502438000000	-2.923608000000
H	8.730906000000	-17.075053000000	-1.557638000000
H	6.895072000000	-18.405283000000	-2.837350000000
H	6.529192000000	-16.910114000000	-3.679388000000
H	4.998490000000	-17.300982000000	-1.744896000000
H	6.364387000000	-17.405146000000	-0.651576000000
H	5.492345000000	-14.905357000000	-2.200030000000
H	5.249447000000	-15.214994000000	-0.492959000000
H	7.828955000000	-15.403328000000	-0.274388000000
H	7.132764000000	-13.795791000000	-0.498363000000
O	8.415676000000	-13.361973000000	-2.556906000000
H	9.000870000000	-17.438842000000	-3.267734000000

B

N	6.836784000000	-8.528323000000	-2.764720000000
N	10.339280000000	-9.887034000000	-1.758912000000
C	7.938243000000	-9.044677000000	-1.879431000000
H	8.016156000000	-8.333116000000	-1.048940000000
H	7.577830000000	-9.999371000000	-1.477777000000
C	9.276650000000	-9.201894000000	-2.590171000000
H	9.182674000000	-9.800749000000	-3.503559000000
H	9.694519000000	-8.226010000000	-2.862936000000
C	11.537489756831	-9.857710291618	-2.674433783775

H	11.803740654749	-8.818740903066	-2.882352655006
H	12.368997327654	-10.359573885628	-2.175252612730
H	11.292057129030	-10.381503552049	-3.601373400198
C	10.372634377347	-9.095363922781	-0.481782854993
H	9.436697742234	-9.229639026311	0.064191257227
H	11.197375747256	-9.465031804692	0.131766105916
H	10.535951331449	-8.040655202020	-0.718490510465
C	5.609717000000	-8.355274000000	-1.899983000000
H	5.834153000000	-7.629948000000	-1.114075000000
H	4.805259000000	-7.990009000000	-2.543651000000
H	5.347644000000	-9.322902000000	-1.464680000000
C	7.171061428948	-7.083210578651	-3.029947093291
H	7.389546669795	-6.593464658919	-2.076927839103
H	8.028648338675	-7.024647596986	-3.704140236412
H	6.292594653231	-6.633083346959	-3.510121459824
C	9.981985000000	-11.318113000000	-1.469076000000
H	9.782396000000	-11.835064000000	-2.411095000000
H	10.829468000000	-11.788867000000	-0.965621000000
H	9.112580000000	-11.363595000000	-0.810996000000
C	6.494713000000	-9.499261000000	-3.863373000000
H	7.325373000000	-9.569176000000	-4.568674000000
H	6.278916000000	-10.473879000000	-3.417376000000
H	5.612849000000	-9.108466000000	-4.380027000000
C	3.785323000000	-6.565121000000	-5.225760000000
C	2.447496000000	-6.767663000000	-5.870761000000
C	1.350279000000	-5.868138000000	-5.279418000000
C	1.365732000000	-4.442963000000	-5.811354000000
C	2.653424000000	-3.682649000000	-5.526797000000
C	3.894055000000	-4.304882000000	-6.128246000000
O	4.419313000000	-5.407131000000	-5.342298000000
H	3.726438000000	-4.649577000000	-7.157527000000
H	2.570918000000	-2.665791000000	-5.929894000000
H	2.813265000000	-3.568969000000	-4.444632000000
H	0.519571000000	-3.891407000000	-5.386462000000

H	1.196622000000	-4.465633000000	-6.898715000000
H	1.430659000000	-5.867627000000	-4.182346000000
H	0.384354000000	-6.329740000000	-5.510576000000
H	2.526554000000	-6.592941000000	-6.953568000000
H	2.202318000000	-7.823136000000	-5.728579000000
O	4.330136000000	-7.434995000000	-4.553741000000
H	4.725422000000	-3.596580000000	-6.144730000000

References

[1] R. Kawai, S. Yada and T. Yoshimura, *ACS Omega*, 2019, **4**, 14242–14250.

[2] S. Sagar, H. Karmakar, P. Nath, A. Sarkar, V. Chandrasekhar and T. K. Panda, *Chemical Communications*, 2023, **59**, 8727–8730.

[3] P. Naert, K. Rabaey and C. V. Stevens, *Green Chemistry*, 2018, **20**, 4277–4286.

[4] Y. Zhao, X. Lim, Y. Pan, L. Zong, W. Feng, C. H. Tan and K. W. Huang, *Chemical Communications*, 2012, **48**, 5479–5481.

[5] S. Sagar, P. Nath, K. Bano, H. Karmakar, J. Sharma, A. Sarkar and T. K. Panda, *ChemCatChem,* **2023**, e202300972.